Electronic Supplementary Material (ESI) for Green Chemistry.

Supplementary Material

Constructing Robust and Recyclable Self-Powered Polysaccharides-Based Hydrogels via Adjusting Zn^{2+}/Li^{+} Bimetallic Networks

Qi Zhou[1], Weijun Yang[1]*, Shengxu Lu[1], Debora Puglia[2], Daqian Gao[3], Pengwu Xu[1], Yunpeng Huang[1], Tianxi Liu[1], Li Wu[1], Chenjing Huang[1], Piming Ma[1]*

[1], The Key Laboratory of Synthetic and Biological Colloids, Ministry of Education, School of Chemical and Material Engineering, Jiangnan University, Wuxi, 214122, China.

[2], Civil and Environmental Engineering Department, Materials Engineering Center, Perugia University, UdR INSTM, Terni 05100, Italy

[3], Department of Surgery, School of Medicine, Yale University, New Haven, 06510, USA.

Corresponding authors: weijun.yang@jiangnan.edu.cn; p.ma@jiangnan.edu.cn.

Table of contents:

Figure S9. The illustrative diagram of the self-powered hydrogel battery charging multiple capacitors.

Figure S10. The illustrative diagram of self-powered hydrogel batteries still outputs normal voltage when subjected to mechanical damage.

Table S1. The application performance of our work was compared with that of other similar hydrogels.

Materials

Microcrystalline cellulose (MCC, TLC) was purchased from Sinopharm Chemical Reagent Co., Ltd. Carboxymethyl chitosan (CMCS, substitution degree: ≥80%), and polyvinyl alcohol (PVA, 1799, alcoholysis degree: 98-99%) were purchased from Shanghai Macklin Biochemical Technology Co., Ltd. Sodium alginate (SA, AR), sodium periodate ($NaIO_4$, 99.5%), Zinc sulfate heptahydrate ($ZnSO_4.7H_2O$, 99.5%), and lithium chloride (LiCl, 99%) were purchased from Beijing InnoChem Science & Technology Co., Ltd. All other reagents were of analytical grade and used as received. Deionized water was used in all experiments.

Preparation of Cellulose Nanocrystals (CNC) and Dialdehyde Sodium Alginate (DSA)

Cellulose nanocrystals (CNC) were prepared using the sulfuric acid hydrolysis method. Briefly, 1 g of microcrystalline cellulose was mixed with 20 mL of 64% sulfuric acid solution. The mixture was stirred vigorously at a constant temperature of 50 °C for 1 h in a water bath. Afterward, it was centrifuged and washed until the pH within the range of 6-7 of supernatant. The obtained suspension was dialyzed for three days to purify it, followed by freeze-drying for 72 hours to obtain CNC.

Dialdehyde sodium alginate (DSA) was prepared using the sodium periodate oxidation method and undergoes a simple modification.[1] Briefly, 2 g of sodium alginate was dissolved in 98 mL of deionized water under stirring at room temperature. Then, the sodium periodate solution was slowly added with stirring. The reaction was carried out under at 30°C for 6 h while avoiding light. The molar ratio of sodium alginate to sodium periodate was 1:1. Afterward, 5 mL of ethylene glycol was added to quench the reaction. After the reaction, the solution was purified using dialysis bags for 3 days, followed by freeze-drying to obtain DSA.

Characterization

The moisture content (MC) and density (DS) of the hydrogels were calculated according to the following formulas, $MC=(M_1-M_2)/M_1$, $DS=M_2/V$, respectively. Where M_1 is the weight of the hydrogel before drying in a 60 °C oven, M_2 is the weight of the hydrogel after drying in a 60 °C oven, and V is the volume of the hydrogel before drying, respectively. The rheological performance of the hydrogel was tested at room temperature using a rotational rheometer (MCR302e, Anton Paar) with a strain of 1% and a frequency range of 0.1-100 rad/s. The morphology of the freeze-dried hydrogels was examined using field-emission scanning electron microscopy (SEM) (S4800, Hitachi) at an accelerating voltage of 5 kV. Energy Dispersive X-ray Spectroscopy (EDS) analysis can be conducted on the same instrument. The FT-IR spectra of the hydrogels were obtained using ATR/FT-IR (Nicolet iS50, Thermo Fisher) with a scanning range of 600-4000 cm^{-1}, a resolution of 4 cm^{-1}, and 32 scans, respectively. The Raman spectra of the hydrogel were recorded using a microscopic confocal Raman spectrometer (Renishaw, InVia) with an excitation wavelength of 532 nm in the scanning range of 4000-400 cm^{-1}. The freezing point of the hydrogels were determined using differential scanning calorimetry (DSC) (DSC3, Mettler Toledo). The sample temperature was subjected to a gradient, first cooling from 30 °C to -65 °C at a rate of 5 °C/min, followed by holding at -65 °C for 10 minutes, and then heating back to 30 °C at a rate of 5 °C/min. The X-ray diffraction (XRD) patterns were performed with an X-ray diffractometer (D8, Bruker AXS) with Cu-K_{α} radiation (λ = 1.5406 Å, 40 kV, 20 mA) with a scanning range of 5-50° and a scanning rate of 4 °/min. High-resolution X-ray photoelectron spectroscopy (XPS) spectra of freeze-dried hydrogels were obtained in the form of binding energy by XPS (AXIS Supra, Kratos) using an AlK_{α} radiation as X-ray source to investigate the influence of ions on hydrogel structure. All spectrums were calibrated by C 1s (284.8 eV).

Sensing Measurements

The relative resistance change (ΔR) of the hydrogels were measured at different strains (1%, 2%, 10%, 25%, 50%, 100%, and 200%) through the utilization of both the electrochemical workstation and the universal mechanical testing machine. The sensitivity gauge factor (GF) of the hydrogels was determined by the following formula: $GF=\Delta R/\varepsilon$, ε represents the applied strain. Furthermore, the hydrogels were subjected to over 1000 cycles of compression at 25% and 50% strain to evaluate the signal stability during practical usage.

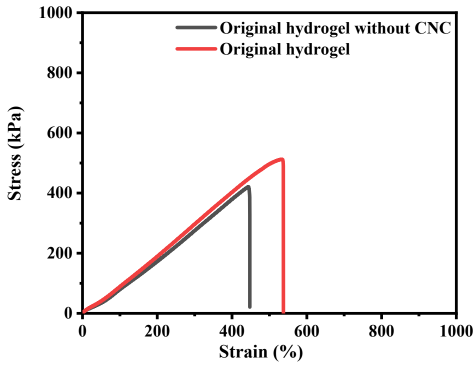

Figure S1. Stress-strain curves of original hydrogel and original hydrogel without CNC.

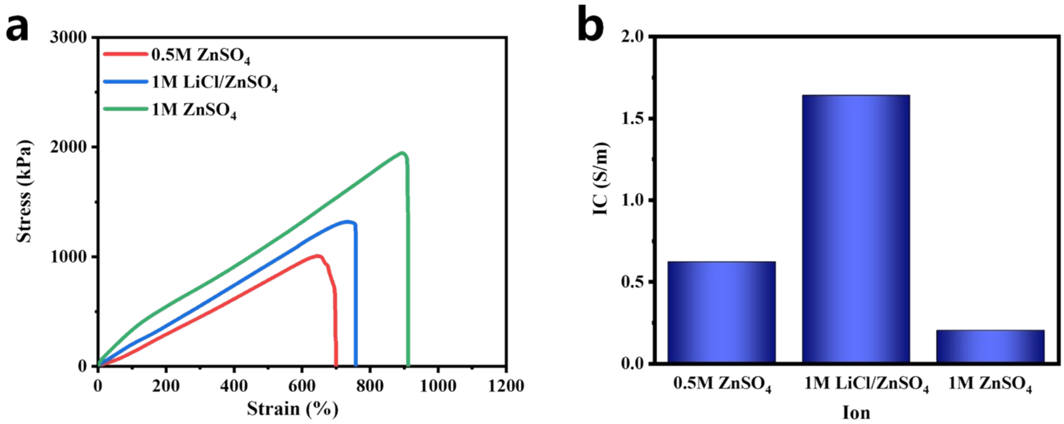

Figure S2. Stress-strain curves (a) and ionic conductivity (b) of hydrogels equilibrated in 0.5M zinc sulfate solution, 1M Zn^{2+}/Li^{+} bimetallic salt solution and 1M zinc sulfate solution.

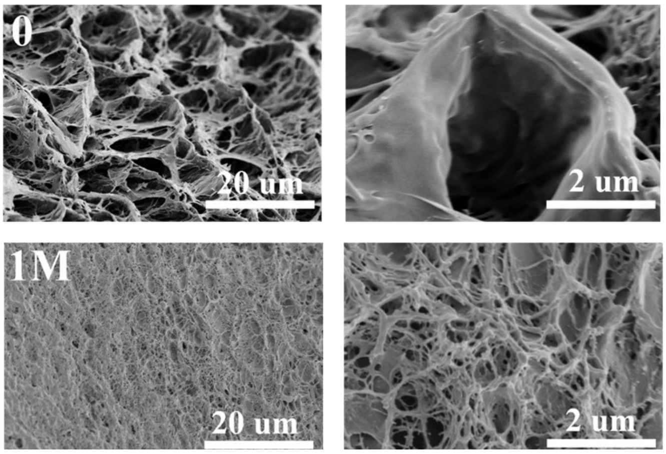

Figure S3. Microscopic morphology of the original hydrogel and hydrogel at 1M concentration.

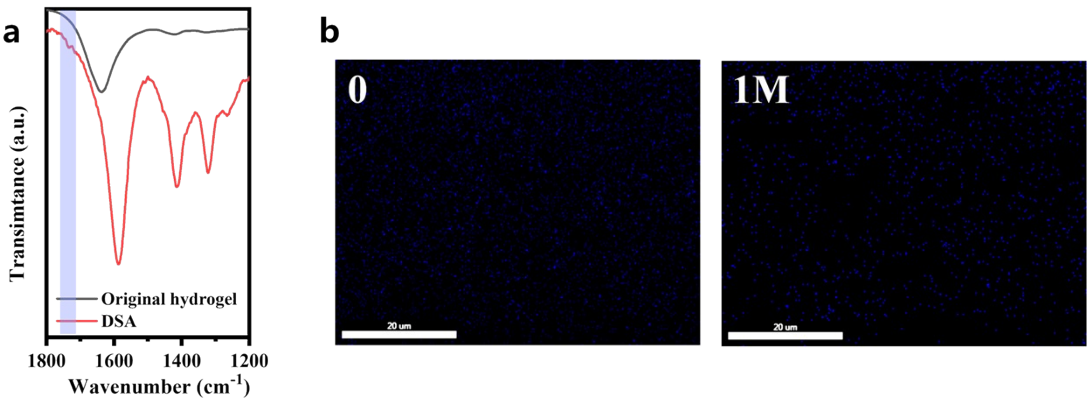

Figure S4. ATR-FTIR spectra (a) of DSA and original hydrogel and EDS spectrum (b) of B element of the original hydrogel and hydrogel at 1M concentration.

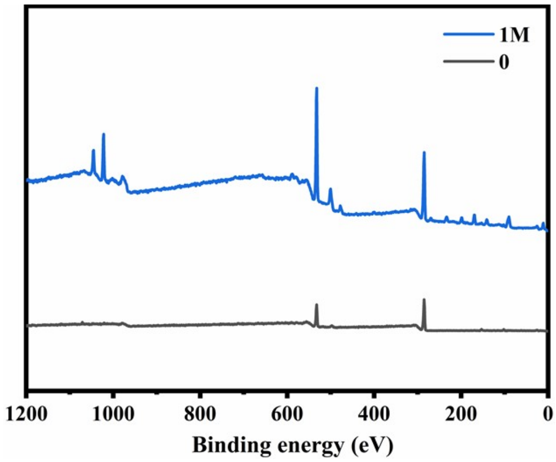

Figure S5. The XPS spectra of the original hydrogel and hydrogel at 1M concentration.

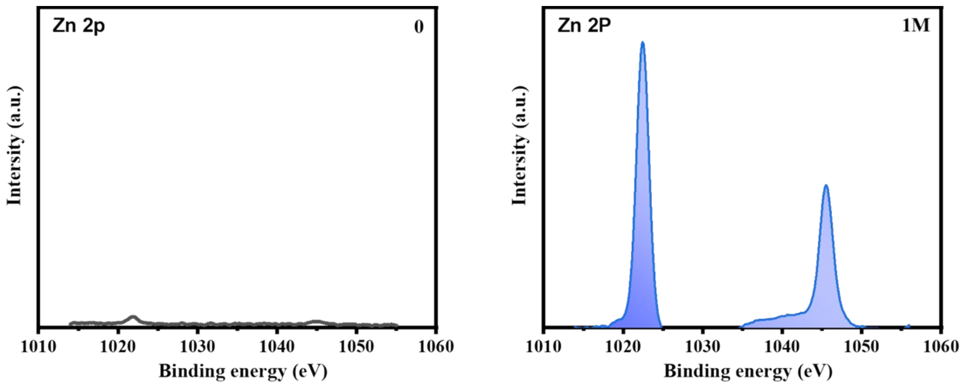

Figure S6. The Zn 2p XPS spectra of the original hydrogel and hydrogel at 1M concentration.

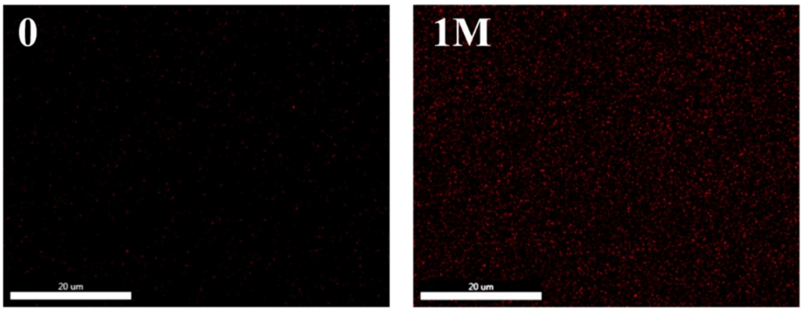

Figure S7. The EDS spectrum of Element Zn of the original hydrogel and hydrogel at 1M concentration.

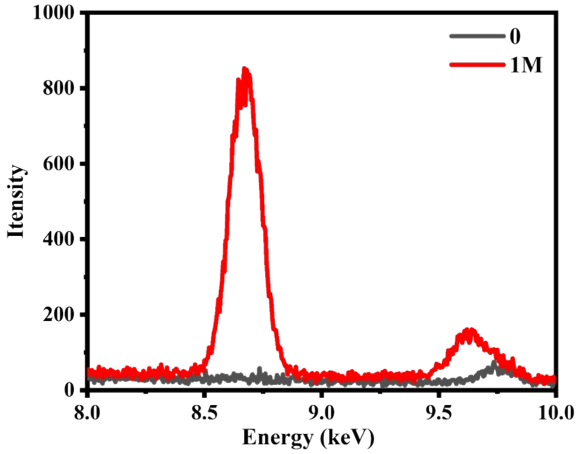

Figure S8. The EDS spectrum analysis of element Zn of the original hydrogel and hydrogel at 1M concentration.

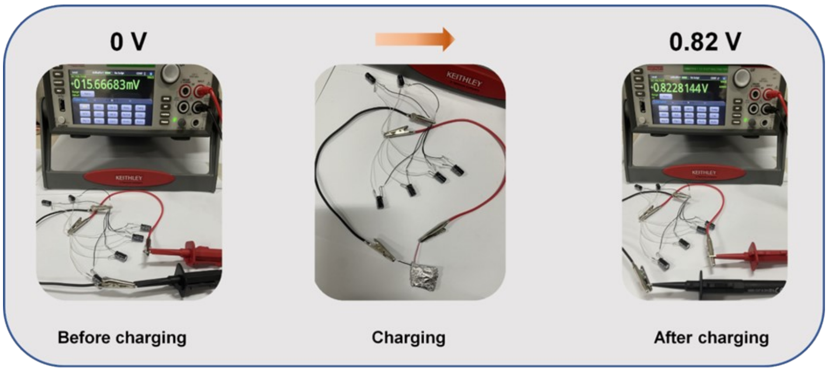

Figure S9. The illustrative diagram of the self-powered hydrogel battery charging multiple capacitors.

Figure S10. The illustrative diagram of self-powered hydrogel batteries still outputs normal voltage when subjected to mechanical damage.

Table S1. The application performance of our work was compared with that of other similar hydrogels.

Sample	Ion	TS (MPa)	Conductivity (S/m)	The output voltage（V）	Stability	Charge	Environmental stimulation	Recyclability	Reference
PVA/PAMAA	NaCl	0.34	1.31	0.66	√	Yes	No	√	[2]
PVA	LiCl	0.1	1.5	1	√	Yes	No	√	[3]
Gelatin/AM/AA	$(NH_4)_2SO_4$	0.14	2.5	0.92	√	No	No	-	[4]
CS/PAAm/PAAc/TA	$ZnCl_2$	~0.27	-	0.90	√	No	No	-	[5]
PAM/AMPS	LiCl	-	-	0.81	-	No	Yes	√	[6]
PVA/PAAM	$K_4[Fe(CN)_6]$/$K_3[Fe(CN)_6]$/KCl	0.30	1.71	0.015	-	No	Yes	-	[7]
PAAM/CMC/TA	$ZnSO_4$/$MnSO_4$	1.32	0.76	1.46	√	Yes	No	√	[8]
PHEA	$(NH_4)_2SO_4$	0.16	2.64	-	√	Yes	No	√	[9]
PAM/XG/SA	LiCl/M^{n+}	~0.62	-	0.8	-	No	No	-	[10]
PVA/P(AM-co-SBMA)	$ZnCl_2$	0.315	1.57	0.86	-	No	No	-	[11]
PVA/CMCS/DSA/CNC	LiCl/$ZnSO_4$	1.36	1.64	0.82	√	No	No	√	**This work**

References

1. J. Chen, S. Li, Y. Zhang, W. Wang, X. Zhang, Y. Zhao, Y. Wang and H. Bi, *Advanced Healthcare Materials*, 2017, **6**, 1700746.
2. J. Huang, S. Peng, J. Gu, G. Chen, J. Gao, J. Zhang, L. Hou, X. Yang, X. Jiang and L. Guan, *Materials Horizons*, 2020, **7**, 2085-2096.
3. Q. Rong, W. Lei, J. Huang and M. Liu, *Advanced Energy Materials*, 2018, **8**, 1801967.
4. X. Zou, X. Wang, Z. Bai, O. Yue, C. Wei, L. Xie, H. Zhang and X. Liu, *Chemical Engineering Journal*, 2023, **463**, 142349.
5. Z. Bi and W. Yuan, *Composites Part A: Applied Science and Manufacturing*, 2023, **175**, 107756.
6. H. Zhang, N. He, B. Wang, B. Ding, B. Jiang, D. Tang and L. Li, *Advanced Materials*, 2023, **35**, 2300398.
7. J. Li, Z. Wang, S. A. Khan, N. Li, Z. Huang and H. Zhang, *Nano Energy*, 2023, **113**, 108612.
8. Y. Li, R. Miao, Y. Yang, L. Han and Q. Han, *Soft Matter*, 2023, **19**, 8022-8032.
9. J. Yang, B. Zhang, X. Tian, S. Liu, Z. Xu, G. Sun, G. Qin and Q. Chen, *Journal of Materials Chemistry C*, 2022, **10**, 17675-17683.
10. T. Li, H. Wei, Y. Zhang, T. Wan, D. Cui, S. Zhao, T. Zhang, Y. Ji, H. Algadi, Z. Guo, L. Chu and B. Cheng, *Carbohydrate Polymers*, 2023, **309**, 120678.
11. Z. Zhou, Z. He, S. Yin, X. Xie and W. Yuan, *Composites Part B: Engineering*, 2021, **220**, 108984.